PERIODICA POLYTECHNICA SER. EL. ENG. VOL. 42, NO. 4, PP. 427-449 (1998)

TRIPLE-POLE BRAKING OF CAGE INDUCTION MOTORS IN AC DRIVES

M. N. ABDEL-HAMID, Azza M. ABDEL-HAMID and M.O. KHALIL

Electrical Engineering
Power Department
Cairo University
Cairo, Egypt

Received: June 30, 1997

Abstract

The presented triple-pole braking method is based on operating the 3-phase cage induction motor from a l-phase supply and utilizing the third-harmonic air-gap mmf wave produced by reconnection of the stator phases in series or in parallel. This results in a braking motor torque in the range from the fundamental synchronous speed to one-third of this speed, where mechanical brake is to be applied to stop the motor. This presented method competes successfully with the methods in present industrial use in respect of electrical energy consumption during the braking process, simplicity of switching, and saving in space and cost.

Keywords: cage motor braking methods, triple-pole braking.

List of Principal Symbols

En_1	=	Kinetic energy at fundamental syn. speed, Watt-sec.
f_1	=	Supply frequency, Hz.
I_{ac}	=	Polyphase current equivalent to DC braking current.
I_p, I_n, I_z	=	Positive-, negative-, and zero-sequence current components.
I_z	=	Stator current in triple-pole operation.
I_{fi3}, I_{fo3}	=	Referred inner- and outer-cage currents of forward field on triple-pole operation.
I_{bi3}, I_{bo3}	=	Referred inner- and outer-cage currents of backward field on triple-pole operation.
J	=	Moment of inertia of rotating masses. N.m.sec^2.
$n_1, n_1/3$	=	Fundamental and triple-pole syn. speeds, rpm.
n	=	Actual motor speed.
P	=	Number of pole pairs.
R_1	=	Stator resistance per phase. Ohm.
R_2	=	Referred rotor resistance of a l-cage motor.
R_{i3}, R_{o3}	=	Referred inner- and outer-cage resistances per phase on triple-pole operation.

R_{eq} = Equivalent resistance: $R_{i3} \cdot R_{o3}/(R_{i3} + R_{o3})$
s = Per-unit slip referred to fundamental syn. speed.
s_f, s_b = Forward and backward slip on triple-pole operation referred to $n_1/3$.
T_f, T_b, T_{3p} = Forward, backward, and resultant torques on triple-pole operation.
T_p, T_n, T_z = Sequence torques with asymmetrical connections.
V_p, V_n, V_z = Sequence voltages per phase.
X_1 = Stator leakage reactance per phase, Ohm.
X_i, X_{2c} = Referred inner-cage and common leakage reactances on normal operation.
X_{i3}, X_{2c3} = Referred inner-cage and common-leakage reactances on triple-pole operation.
X_m = Magnetizing reactance on normal operation.
X_{m3} = Magnetizing reactance on triple-pole operation.
Z_p, Z_n, Z_z = Positive-, negative-, and zero-sequence phase impedances.
ω_1, ω_3 = Angular speeds corresponding to n_1 and $n_1/3$, mechanical radians/sec.

1. Introduction

In AC induction-motor drives, various braking methods are presently applied industrially. A well-known and straightforward method is 'counter-current' braking usually named 'plugging', in which the voltage phase sequence at the motor terminals is reversed to start the braking process. Other methods include DC dynamic braking [4,7] and many asymmetrical connections [9].

In this paper, the presented so-called triple-pole braking method is investigated. To realize where this method stands, it becomes necessary to make a comparison with the following most common types of braking used in connection with induction motors:

a) Plugging.
b) DC dynamic.
c) Siemens' braking connection, representing an important method of many asymmetrical connections in use.

The above four methods for braking will be compared essentially on the basis of the energy loss involved in the rotor and motor circuits during the braking process; of course, safety and cost being also important. Economy in energy is considered the most important factor, since nowadays it is universally aimed at. Consequently, theoretical expressions for the energy dissipated shall be developed, using certain simplifying assumptions which do not affect their validity.

It may be noted that considerations of safety make it desirable, if not essential, to fit also a mechanical brake to most industrial drives: such a brake is usually rated at about 100% of the full-load motor torque. Normally, it is cheap, but requires maintenance and readjustment for satisfactory operation.

2. Theory of Triple-Pole Braking

2.1. Theory and Equivalent Circuit

The scheme of triple-pole operation presented here applies a principle normally disregarded, namely operation of the motor on a harmonic field, which is specifically the third harmonic; multiples of three being ignored for insignificance. The method is applicable to cage motors only since the rotor cage accepts mmf waves having any number of poles set up by the stator windings in the air gap of the machine and reacts by a similar wave of the same number of poles, with all other rotor mmf waves cancelled out [2].

To obtain triple-pole mmf wave by the stator which is normally wound for 3-phase operation, the windings of the three stator phases, originally connected in star or delta, are reconnected in series or in parallel, as shown in *Fig. 1*, and fed from a 1-ph supply. The 3-phase currents will then be all equal and in phase, i.e. they form together a zero-sequence system according to the symmetrical components terms. In the series connection the currents are lower and the zero-sequence phase voltage V_z will be $V/3$, where V is the applied 1-phase voltage.

With the scheme described above, the induction motor is effectively a 1-ph induction motor with triple-pole air-gap field, the equivalent circuit on such operation is expectedly similar to that of the 1-ph motor, with one branch representing the forward-rotating field component of the pulsating air-gap field, and the second branch for the backward-rotating component. The p.u. slip values of the motor w.r.t. these fields are called s_f and $(2-s_f)$, respectively, referred to the triple-pole synchronous speed, $n_1/3$, where n_1 is the fundamental synchronous speed. If these slip values are expressed in terms of the slip 's' referred to n_1, their values will be $(3s-2)$ and $(4-3s)$, respectively. In *Figs. 2a* and *2b* the equivalent circuits of the test motor are drawn, a 2-cage motor was available on normal 3-ph operation and on triple-pole 1-ph operation (which may also be called zero-sequence operation). The parameters of the former circuit were experimentally determined by a devised method, while those of *Fig. 2b* were concluded from the corresponding values [1,2,6] of *Fig. 2a*; all parameters are given in Appendix for the test motor. Such derivation of parameters requires a lengthy separate investigation which is beyond the scope of this paper dedicated to presentation of the triple-pole braking method. However, the validity of

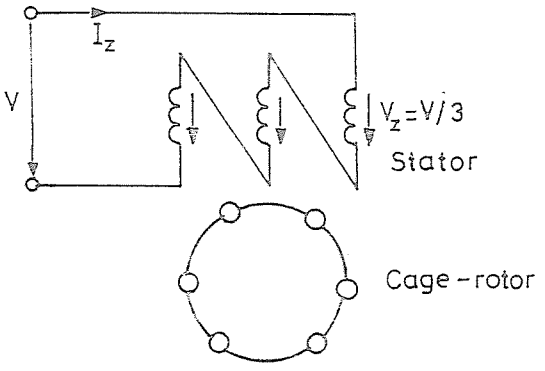

a) Series connection

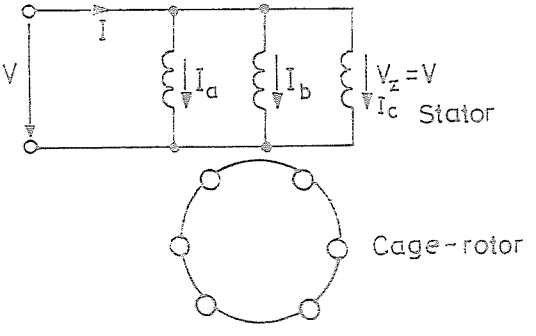

b) Parallel connection

Fig. 1. Triple-pole connections

these equivalent circuits was proved by the satisfactory agreement between computations and measurements, as seen in *Figs. 3* to *6*.

Figs. 3 and *4* show the I/n and T/n characteristics on normal 3-ph operation with the rated voltage of 380 volt, and *Figs. 5* and *6* show the same curves on triple-pole operation with a 1-ph voltage of 380 volt, which is the same available line voltage in order to avoid any necessary extra equipment. The tests were carried out by setting a Ward-Leonard speed control scheme, *Fig. 7*, with the field current of the calibrated DC machine coupled to the test motor kept constant, and that of the DC machine of the auxiliary set varied to achieve the required speed of the test motor. Computed torques were corrected for the stray-loss torque, which is due to the stray loss. This loss was measured by the 'reverse rotational' method recommended by the American 'AIEE Committee' report for all sizes and

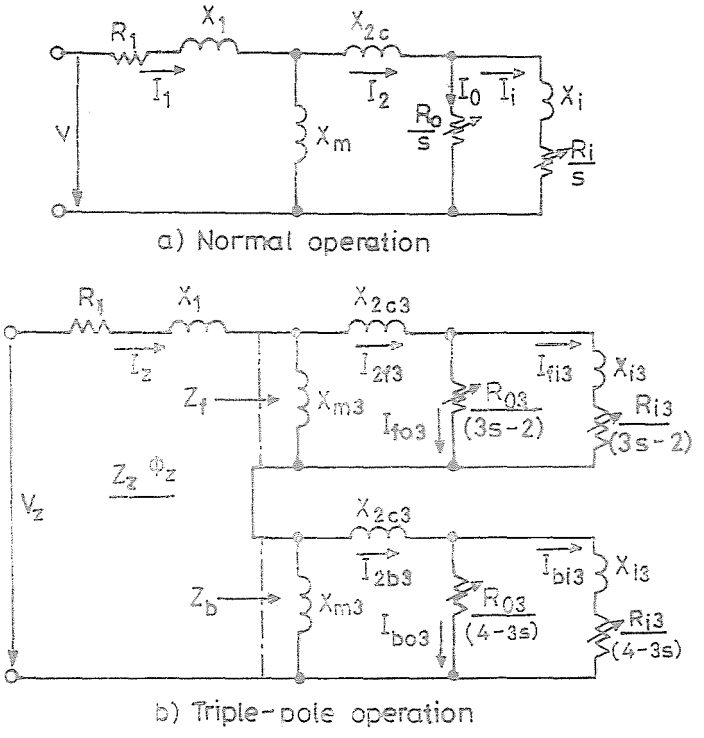

Fig. 2. Equivalent-circuits of the double-cage induction motor

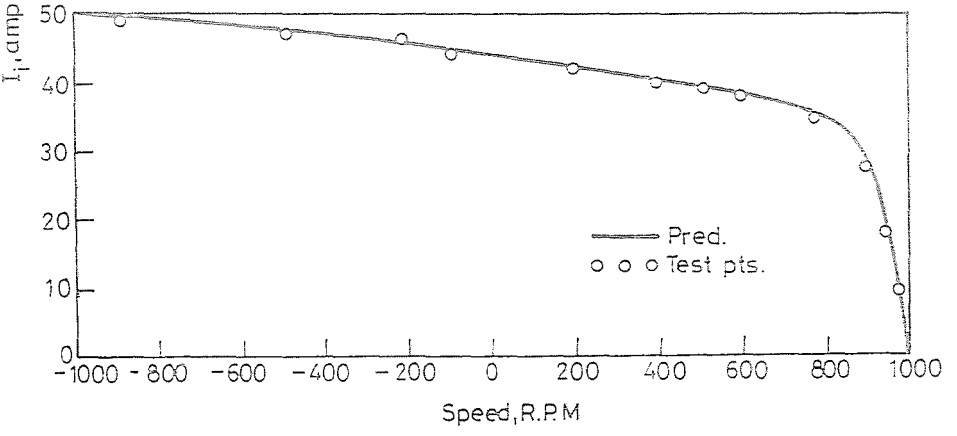

Fig. 3. I_1/n curve of test motor ($V_{ph} = 220$)

constructions of cage motors (9).

In brief, such stray loss is the loss remaining after all other known losses considered. They are mainly iron losses occurring both in the stator

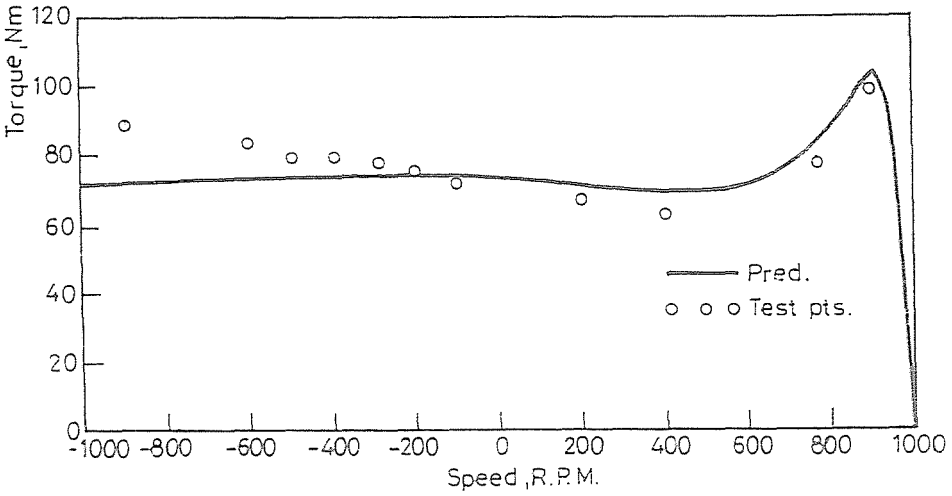

Fig. 4. T/n curve of test motor ($V_{ph} = 220$)

and rotor due to tooth pulsations attributed to the variation of air-gap permeance caused by slotting and stator winding distribution. The general effect of the stray-loss torque is like that of the friction torque, meaningly it is subtracted from the motor developed torque in the motoring region, and added to it in the braking region.

2.2. Performance Calculation

With reference to *Fig. 2b*, and applying the series connection of *Fig. 1a*, the current and total power are given by:

$$I_z = \frac{V_z}{Z_z} \tag{1}$$

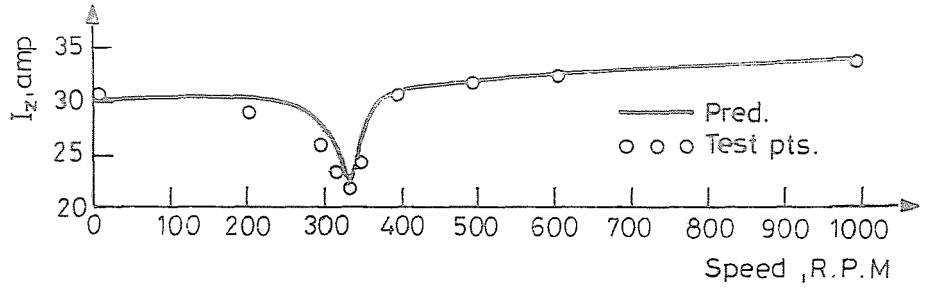

Fig. 5. I_2/n curve of test motor on triple-pole operation ($V_z = 380/3$)

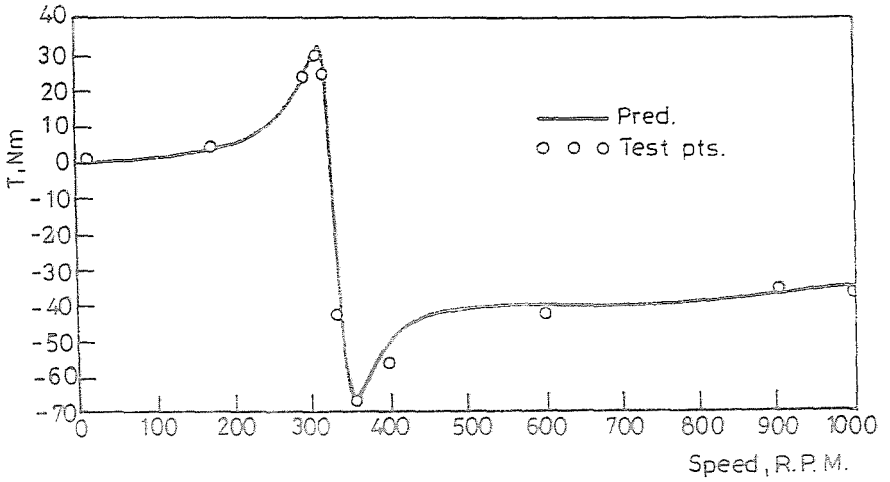

Fig. 6. T/n curve of test motor on triple-pole operation ($V_z = 380/3$)

and

$$P_z = 3 \cdot V_z \cdot I_z \cdot \cos \varphi_z. \tag{2}$$

The impedance Z_z can be calculated at any slip from the equivalent circuit of *Fig. 2b*. As for the torques, the forward, backward, and net torque on triple-pole operation are given by:

$$T_f = 3 \cdot \left[I_{fi3}^2 \cdot \frac{R_{i3}}{(3s-2)} + I_{fo3}^2 \cdot \frac{R_{o3}}{(3s-2)} \right], \tag{3}$$

Syn. Watts r.t. $\frac{n_1}{3}$

$$T_b = 3 \cdot \left[I_{bi3}^2 \cdot \frac{R_{i3}}{(4-3s)} + I_{bo3}^2 \cdot \frac{R_{o3}}{(4-3s)} \right], \tag{4}$$

Syn. Watts r.t. $\frac{n_1}{3}$

$$T_{3p} = (T_f - T_b). \tag{5}$$

It is obvious that the starting torque, $s = 1$, has a zero value. Also it is noted that T_f is positive and higher than T_b below $n_1/3$, 's' higher than $2/3$, i.e. the triple-pole torque is positive below $n_1/3$, being of small negative value at exactly this speed. Beyond this speed, T_f will be a generating torque, while T_b will still be a braking torque and, therefore, they add up to yield a resultant braking torque.

As for the mechanical power developed by the forward- and backward-rotating fields, they may be expressed as follows:

$$P_{mf} = T_f \cdot (1 - s_f)$$

$$= \quad 3 \cdot T_f \cdot (1-s), \qquad \text{Watts.} \tag{6}$$

and similarly:

$$P_{mb} \quad = \quad -3 \cdot T_b \cdot (1-s), \qquad \text{Watts.} \tag{7}$$

Therefore, the resultant mechanical power on triple-pole operation will be:

$$P_{m,3p} \quad = \quad 3 \cdot (1-s) \cdot (T_f - T_b), \qquad \text{Watts.} \tag{8}$$

It is obvious that the T/n characteristic on triple-pole operation is a braking torque in the range from normal synchronous speed n_1 to a speed slightly less than one-third of this speed, say $(n_1/3)$.

2.3. Energy Dissipated in Motor Circuits during Braking

To start with, a formula is derived for the energy dissipated in the rotor circuit during acceleration from standstill to full speed against an inertia load. The following dynamic equation is valid:

$$T = J \cdot \frac{\mathrm{d}\omega}{\mathrm{d}t}, \tag{9}$$

where: T = acceleration torque, N.m.
J = moment of inertia of rotating masses, N.m.sec^2.
ω = $(1-s)\omega_1$, where ω_1 is the synchronous angular speed in mechanical radians/sec.

Since: $T = P_g/\omega_1$, P_g being the air-gap power in Watts, Therefore:

$$\frac{P_g}{\omega_1} \quad = \quad -J \cdot \omega_1 \cdot \frac{\mathrm{d}s}{\mathrm{d}t}$$

or:

$$s \cdot P_g \cdot \mathrm{d}t \quad = \quad -J \cdot \omega_1^2 \cdot s \cdot \mathrm{d}s. \tag{10}$$

Therefore the energy dissipated in the rotor circuits during acceleration to n_1 is:

$$En_1 \quad = \quad -J \cdot \omega_1^2 \cdot \int_1^0 s\,\mathrm{d}s,$$

$$En_1 \quad = \quad 1/2 \cdot J \cdot \omega_1^2, \qquad \text{watt-sec.} \tag{11}$$

which is equal to the kinetic energy at full synchronous speed.

Now considering the triple-pole operation, and referring to *Fig. 2b*, modified to correspond to a single-cage rotor with referred rotor resistance $= R_2$, we may assume that X_{m3} is large compared with rotor impedance,

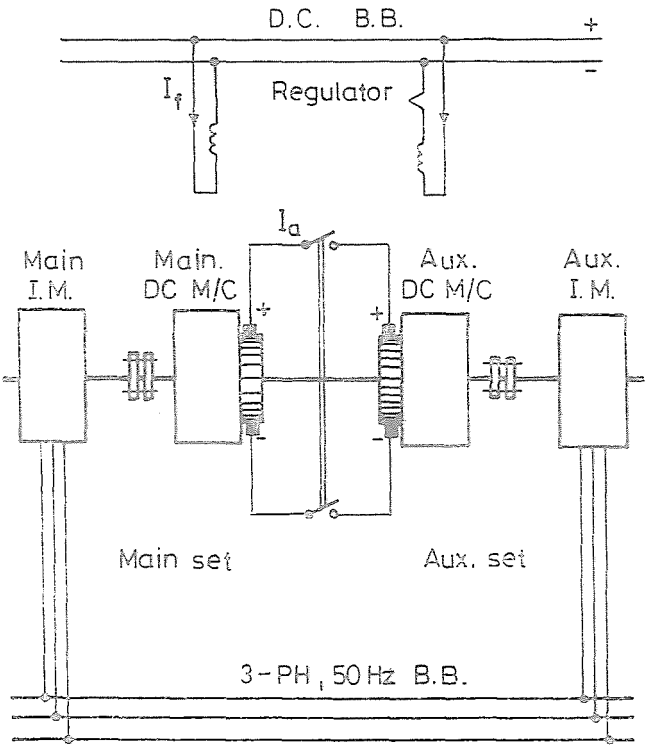

Fig. 7. Test set-up

then the following expression follows from *Eq.* (9) for the braking torque $T_{br} = T_{3p}$:

$$T_{3p} = T_{br} = T_f - T_b = 3 \cdot I_z^2 \cdot R_2 \cdot \frac{1/s_f - 1/(2 - s_f)}{\omega_3} = J \cdot \frac{\mathrm{d}\omega}{\mathrm{d}t}, \qquad (12)$$

where ω_3 = angular synchronous speed at $n_1/3$. and I_z = stator current. Since:

$$\omega = (1 - s_f) \cdot \omega_3,$$

therefore: $\mathrm{d}\omega = -\omega_3 \cdot \mathrm{d}s_f$; *Eq.* (12) is modified to:

$$T_{br} = 3 \cdot I_z^2 \cdot R_2 \cdot \frac{1/s_f - 1/(2 - s_f)}{\omega_3} = -J \cdot \omega_3 \cdot \frac{\mathrm{d}s_f}{\mathrm{d}t}. \qquad (13)$$

Or:

$$3 \cdot I_z^2 \cdot R_2 \cdot \mathrm{d}t = \left[-J \cdot \omega_3^2 \cdot \frac{\mathrm{d}s_f}{\frac{1}{s_f} - \frac{1}{(2-s_f)}} \right]. \qquad (14)$$

The left-hand side multiplied by 2 represents the total copper losses, then the total energy dissipated in the rotor during the braking period from s_{f1} to s_{f2} is found by integrating the right-hand side between these slip values, and multiplying by 2, therefore:

$$2 \cdot \int (3 \cdot I_z^2 \cdot R_2) \cdot \mathrm{d}t = -2 \cdot J \cdot \omega_3^2 \cdot \int_{s_{f1}}^{s_{f2}} \frac{s_f \cdot (2 - s_f)}{(2 - 2s_f)} \cdot \mathrm{d}s_f .$$

Thus:

$$= \frac{J \cdot \omega_3^2}{2} \cdot \left[-s_f^2 + 2s_f + 2\ln(1 - s_f) \right]_{s_{f1}}^{s_{f2}}$$

$$= \frac{J \cdot \omega_3^2}{2} \cdot \left[(s_{f1}^2 - s_{f2}^2) - 2(s_{f1} - s_{f2}) + 2 \cdot \ln \frac{(1 - s_{f2})}{(1 - s_{f1})} \right].$$

∴ Total energy in rotor circuit

$$= \frac{En_1}{9} \cdot \left[(s_{f1}^2 - s_{f2}^2) - (2s_{f1} - s_{f2}) + 2 \cdot \ln \frac{(1 - s_{f2})}{(1 - s_{f1})} \right]. \qquad (15)$$

Referring to *Eq.* (14), and noting that the stator copper losses are $(3I_z^2 \cdot R_1)$, therefore, from *Eq.* (15), the total energy both in stator and rotor circuits during braking between the above limits will be:
Total energy in motor circuits

$$= \frac{En_1}{9} \cdot \left[(s_{f1}^2 - s_{f2}^2) - 2(s_{f1} - s_{f2}) + 2\ln \frac{(1 - s_{f2})}{(1 - s_{f1})} \right] \cdot \left(1 + \frac{R_1}{2 \cdot R_2} \right). \qquad (16)$$

Now, applying *Eq.* (15) between the slip limits $s_{f1} = -2$ and $s_{f2} = 0$, corresponding to speeds n_1 and $n_1/3$ representing the braking range with the slips relative to the triple-pole synchronous speed, we get:
Total energy dissipated in rotor circuit $= 0.64En_1$. (17)
The above two *Eqs.* (15) and (16) relate to motors with 1-cage rotors. However, with 2-cage type, these equations are still applicable, with X_{i3} assumed negligible, and R_2 replaced by R_{eq} given by:

$$R_{eq} = \frac{R_{i3} \cdot R_{o3}}{(R_{i3} + R_{o3})}. \qquad (18)$$

2.4. Braking Time from Full to One-Third Speed

Eq. (9) may be rewritten as follows:

$$\mathrm{d}t = J \cdot \frac{2\pi}{60} \frac{\mathrm{d}n}{T}.$$

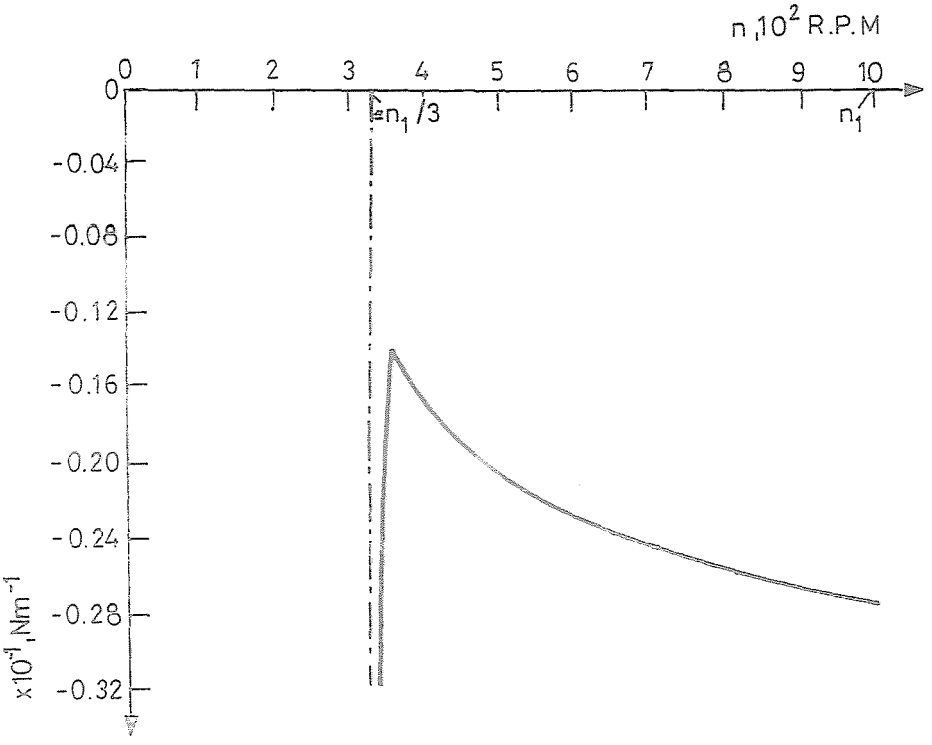

Fig. 8. ($1/T$ vs. n) curve for triple-pole braking

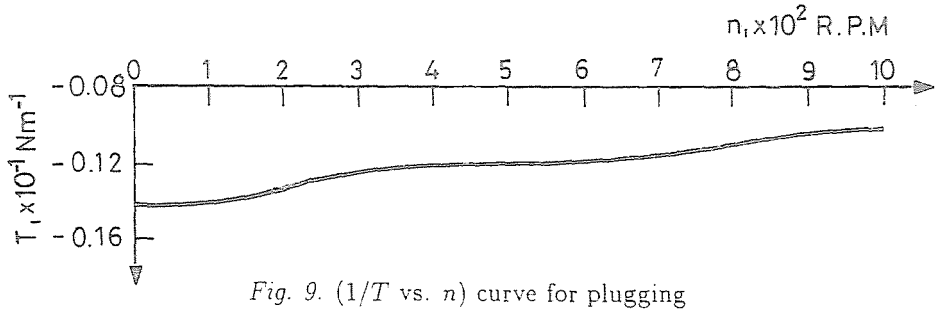

Fig. 9. ($1/T$ vs. n) curve for plugging

Then, in order to calculate the braking period from full-speed n_1 to one-third of this speed, the right-hand side is integrated between these speed limits; therefore:

$$t_{br} = J \cdot \frac{2\pi}{60} \cdot \int_{n_1}^{n_1/3} \frac{\mathrm{d}n}{T}, \qquad \text{sec.} \tag{19}$$

Since there can be no easy expression for the T/n curve of *Fig. 6*, the

required integration of *Eq.* (19) is only practicable by graphical integration of the right-hand side, as in *Fig. 8*. The value of J can be determined by the well-known retardation method.

For the test motor, J was found equal to 3.04 N.m.sec^2, and the braking time to one-third speed, calculated as explained above, was found 5 sec. This result agreed reasonably with the measured value of 4.6 sec.

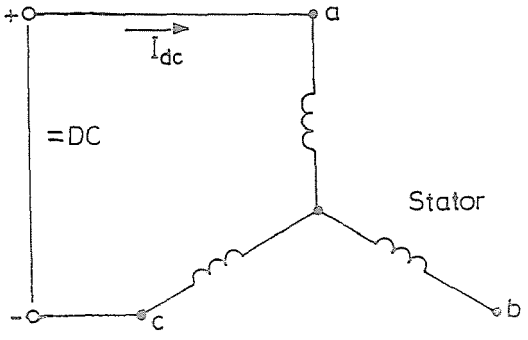

Fig. 10. ($1/T$ vs. n) curve for triple-pole braking

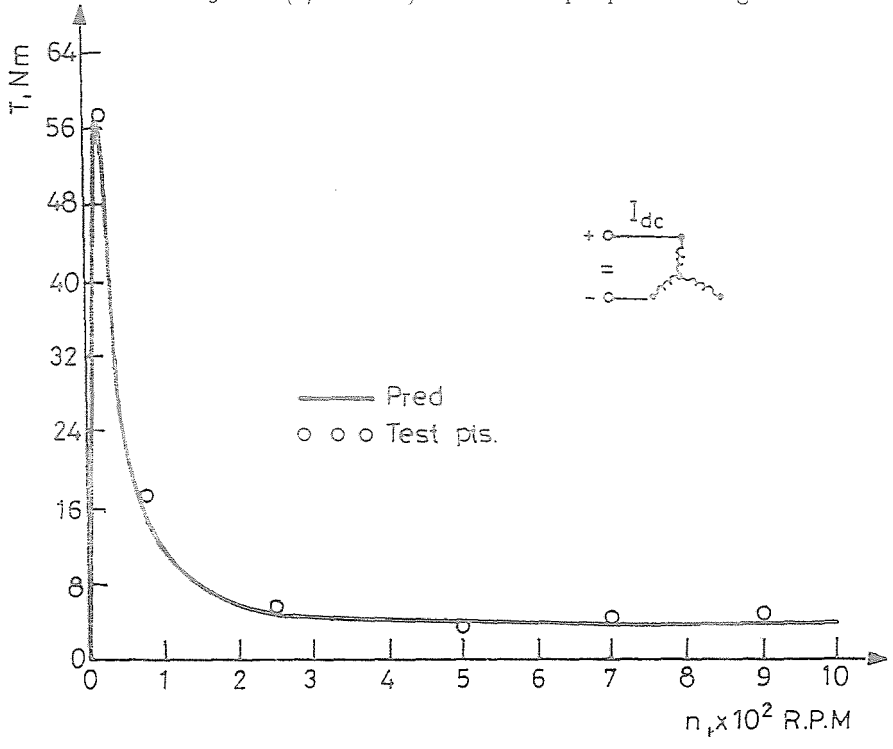

Fig. 11. (T/n vs. n) curve for DC dynamic braking (I_{dc} =12 amp.)

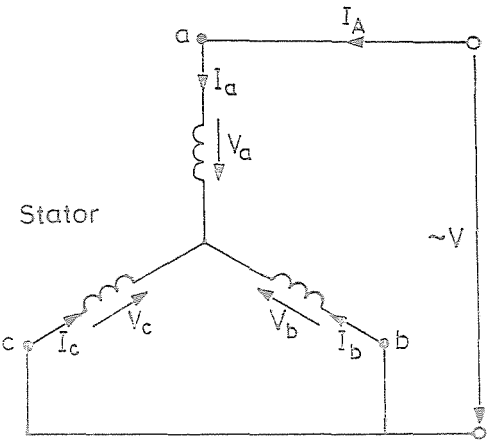

Fig. 12. Siemens' braking connection

Practically, when the motor is brought down to $n_1/3$, the AC supply is removed and instantly the mechanical brake should be applied to dissipate the residual energy of $En_1/9$ to stop the motor.

3. Braking by Plugging

The induction motor runs normally near its synchronous speed within a slip around 5% for normal designs. When braking by plugging is required, two leads feeding the stator terminals are interchanged, thus reversing both the phase sequence of the 3-phase voltage feeding the motor and the direction of rotation of the stator field. The motor will immediately be running at a slip value near 2, i.e. in the braking region, and the motor slows down to standstill, then reverses as a motor if the supply is still on.

3.1. Energy Dissipated in Motor Circuits

The energy dissipated in the rotor circuit during braking is obtained by integrating the right-hand side of *Eq.* (10) between the slip values two and one, with the initial slip on normal operation assumed zero. Therefore:

$$\text{Energy dissipated in rotor circuit} = -J \cdot \omega_1^2 \int_2^1 s\,ds$$

$$= 3 \cdot En_1. \tag{20}$$

Including also the stator losses, the expression will be as follows:

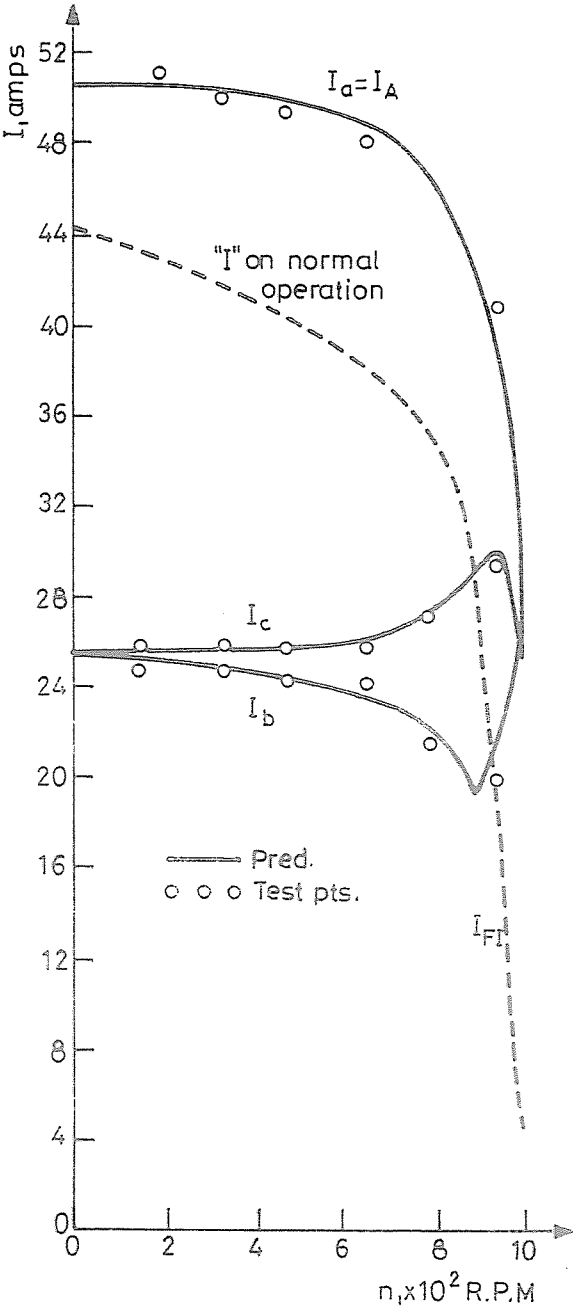

Fig. 13. I/n curves for Siemens' connection ($V = 380$)

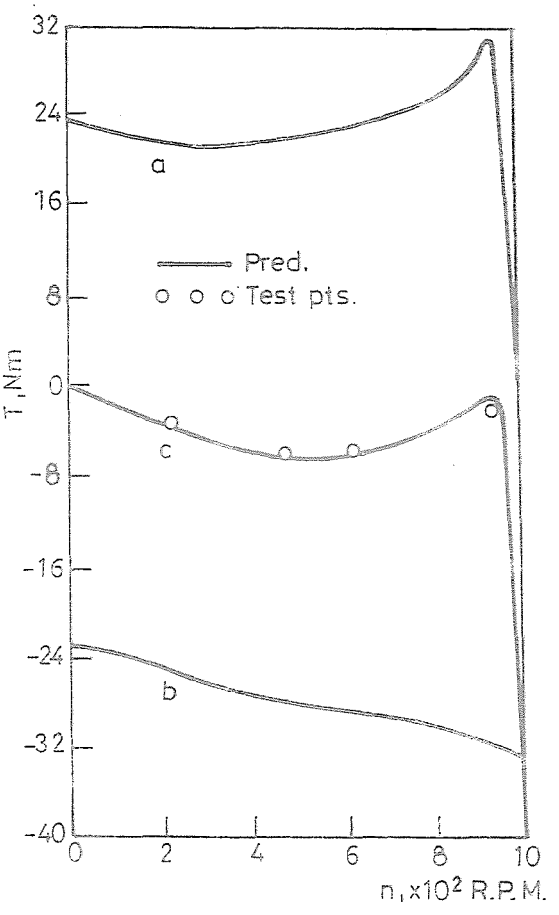

Fig. 14. T/n curve for Siemens' connection (V=380) a) Pos.-sequence ($V_p = V/3$) b) Neg.-sequence ($V_n = V/3$) c) Resultant

$$\text{Energy dissipated in motor circuits} = 3 \cdot En_1 \cdot \left(1 + \frac{R_1}{R_2}\right) \tag{21}$$

and in 2-cage motors, R_2 is replaced by R_{eq} in *Eq.* (18).

3.2. Braking Time

This time is obtained by graphically integrating the right-hand side of *Eq.* (19) applying the ($1/T$ vs. n) curve, between $-n_1$ and $n = 0$, i.e. between $s = 2$ and $s = 1$. The torques in this range are those on normal operation between the given slip limits and the curve of ($1/T$ vs. n) can

easily be drawn as in *Fig. 9.*

The calculated stopping time was found equal to 3.84 sec., and the measured value, found by getting the average of a good deal of stoppings, was 3.5 sec.

4. DC Dynamic Braking

This type of braking has received much attention in practice since it removes the danger of reversal. To start braking when the motor is running at full speed near synchronous speed, the 3-phase AC supply is disconnected, and the stator terminals are then connected to a source of DC supply. Many ways are used practically for this purpose, one of which is shown in *Fig. 10.*

The DC excitation results in a stationary air-gap field which affects the rotor in a way similar to that of a rotating field frozen at a certain instant. On dynamic braking at a speed 'n'. the voltage and current of the rotor are identical to those on normal operation at a speed of $(n_1 - n)$. The torque is a generator torque, i.e. a braking one, with the stator DC current representing the excitation.

4.1. Equivalent Circuit and Performance

The equivalent AC current, I_{ac}, is defined as the polyphase current which will produce in the air gap the same fundamental component of mmf as that produced by the DC excitation on dynamic braking.

For the connection shown in *Fig. 10*, the relation between the two currents will be as follows:

$$I_{dc} = \frac{\sqrt{3}}{\sqrt{2}} \cdot I_{ac}. \tag{22}$$

The equivalent circuit is the same as that on normal operation, *Fig. 2a*, with the slip 's' replaced by 's_b' defined as follows:

$$s_b = \frac{n}{n_1}. \tag{23}$$

Derivations from the equivalent circuit will then be similar to those on 3-phase operation.

A factor that may considerably affect the accuracy of calculations in DC dynamic braking is the wide change in the magnetizing reactance, X_m, with speed since, unlike the case of normal operation, the stator current I_{dc} and its AC equivalent I_{ac} are constant, and in consequence I_m and X_m must keep changing [4]. A new computer programme is designed for performance

calculation with saturation properly considered. The computed T/n curve with a DC excitation current of 12 amp. (equal to normal current of the motor) is shown in *Fig. 11* after being corrected for stray loss torque. It should be noted that the braking torque is low almost in the full speed range from synchronous to standstill except in a small region near zero speed. The shape of the T/n curve could be changed if the motor were a slip-ring one by adding rotor resistances.

4.2. Energy Dissipated in Motor Circuits

Again, applying *Eq.* (10) for the speed range from n_1 to $n = 0$, corresponding to $s_b = 1$ and 0, respectively:

$$\text{Energy dissipated in rotor circuit} = -J\omega_1^2 \cdot \int_1^0 s_b \cdot \mathrm{d}s_b$$

$$= En_1. \tag{24}$$

The total energy in stator and rotor can be expressed as follows:

$$\text{Energy dissipated in motor circuits} = En_1 \left(1 + \frac{R_1}{R_2}\right). \tag{25}$$

As mentioned before, with 2-cage motor R_2 in the above two equations should be replaced by R_{eq}, *Eq.* (18). It is to be noted that *Eq.* (25) gives stator loss which may be considerably less than the actual value with such DC braking.

4.3. Braking Time

Applying graphical integration as previously explained, the calculated braking time with $I_{dc} = 12$ amp. was found 40 sec., the measured value was 24 sec. This discrepancy is attributed to the fact that the braking torque is very low, and comparable with the neglected friction torque. It should be noted that the braking period is too long to be tolerated. However, with slip-ring motors, the T/n curve and the braking period can be adjusted by adding rotor resistances. DC dynamic braking is clearly unsuitable with cage motors.

5. Siemens' Braking Connection

This asymmetrical connection shown in *Fig. 12* is one of many asymmetrical connections applied for braking induction motors. Calculations were carried

out applying the method of symmetrical components, and the following results were obtained, with phase 'a' considered the reference phase:

$$V_z = 0, \tag{26}$$

$$V_p = V_n = \frac{V}{3}, \tag{27}$$

and for the sequence currents:

$$I_z = 0 \tag{28}$$

$$I_p = \frac{V}{3Z_p} \tag{29}$$

$$I_n = \frac{V}{3Z_n}. \tag{30}$$

From the above, the positive and negative sequence torques at any slip 's' have magnitudes equal to one-third of the torques developed at slip values of 's' and $(2 - s)$ on normal operation, respectively.

In *Fig. 13* the phase currents of the test motor are shown against speed; it can be observed that the current I_a, which is also equal to the supply current, is much higher than the current on normal operation and, in consequence, phase 'a' may be overheated. Also, the T/n curve shown in *Fig. 14* yields zero torque at standstill, therefore reversal of rotation does not arise.

5.1. Energy Dissipated in Motor Circuits

In this method of connection, the positive- and negative-sequence voltages are equal, i.e. $V_p = V_n$. Assuming R_2 (of 1-cage rotor) greater than the total leakage-reactance of the motor, and X_m large and negligible, we get:

$$I_p = V_p \cdot \frac{s}{R_2}$$

and

$$I_n = V_p \cdot \frac{(2 - s)}{R_2}. \tag{31}$$

The copper losses in the rotor circuit will be:

$$= 3 \cdot R_2(I_p^2 + I_n^2)$$

$$= 3I_p^2 \cdot R_2 \cdot 2\left(\frac{s^2 - 2s + 2}{s^2}\right). \tag{32}$$

From the dynamic equation:

$$T_p - T_n = J \cdot \frac{\mathrm{d}\omega}{\mathrm{d}t} = -J \cdot \omega_1 \cdot \frac{\mathrm{d}s}{\mathrm{d}t} \tag{33}$$

we obtain:

$$\left[3I_p^2 \cdot \frac{R_2}{s} - 3I_p^2 \cdot \left(\frac{2-s}{s}\right)^2 \cdot \frac{R_2}{2-s}\right] \cdot \frac{1}{\omega_1} = -J \cdot \omega_1 \cdot \frac{\mathrm{d}s}{\mathrm{d}t}$$

$$\therefore 3I_p^2 R_2 \cdot \left(\frac{1}{s} - \frac{2-s}{s^2}\right) \cdot \frac{1}{\omega_1} = -J \cdot \omega_1 \cdot \frac{\mathrm{d}s}{\mathrm{d}t}$$

$$\therefore 3I_p^2 R_2 \cdot \mathrm{d}t = -J \cdot \omega_1^2 \cdot \frac{\mathrm{d}s}{\frac{1}{s} - \frac{2-s}{s^2}}$$

$$= \frac{-J \cdot \omega_1^2}{2} \cdot \frac{s^2}{(s-1)} \cdot \mathrm{d}s. \qquad (34)$$

Referring to *Eq.* (32), it can be seen that the total rotor copper loss is obtained by multiplying both sides of *Eq.* (34) by:

$$2 \cdot \frac{s^2 - 2s + 2}{s^2}.$$

Therefore:

Energy dissipated in rotor circuit

$$= \int_{s_1}^{s_2} \left[\frac{-J\omega_1^2}{2} \cdot \frac{s^2}{(s-1)} \cdot 2 \cdot \frac{s^2 - 2s + 2}{s^2}\right] \mathrm{d}s.$$

The right-hand side gives the energy when braking is performed between the slip limits s_1 and s_2. Carrying out this integration:

Energy in rotor circuit

$$= -J\omega_1^2 \int_{s_1}^{s_2} \left(s - 1 + \frac{1}{s-1}\right) \mathrm{d}s$$

$$= \left(\frac{J\omega_1^2}{2}\right) \cdot \left[s^2 - 2s + 2\ln(s-1)\right]_{s_2}^{s_1}$$

$\therefore$ (Energy dissipated in rotor circuit)

$$= En_1 \left[(s_1^2 - s_2^2) + 2(s_2 - s_1) + 2\ln \cdot \frac{(1-s_1)}{(1-s_2)}\right]. \qquad (35)$$

It follows that:

Energy dissipated in motor circuits, (stator and rotor):

$$= En_1 \cdot \left[(s_1^2 - s_2^2) + 2(s_2 - s_1) + 2\ln \frac{(1-s_1)}{(1-s_2)}\right] \cdot \left(1 + \frac{R_1}{R_2}\right). \qquad (36)$$

As previously explained, for the 2-cage motor R_2 is replaced by R_{eq}, *Eq.* (18).

In this asymmetrical braking connection, it is evident from *Eqs.* (35) and (36) that the energy dissipated in the motor circuits increases indefinitely as the speed approaches zero, i.e. $s_2 = 1$, because of the assumed fictitious case of zero friction-torque. However, it can be reasonably assumed that the AC supply to the motor is disconnected and instantly the mechanical brake applied when the speed has fallen to, say, 10% of the synchronous speed. Then from *Eq.* (35):

$$\text{Energy dissipated in rotor circuit (from } n_1 \text{ to } n_1/10) = 5.605 E n_1. \qquad (37)$$

But for fair comparison with the triple-pole braking, this energy is once more calculated assuming the mechanical brake applied at one-third of the synchronous speed:

$$\text{Energy dissipated in rotor circuit (from } n_1 \text{ to } n_1/3) \quad = 3.09 E n_1. \qquad (38)$$

5.2. Braking Time

By graphical integration, the braking time for the test motor was calculated and found to be 62 sec., the measured value was 40 sec. Again here as with DC dynamic braking, the discrepancy is attributed to neglecting the friction torque which is comparable with the low resultant braking torque with this asymmetrical connection.

It should be noted that the braking time is too high to be accepted when cage motors are dealt with. However, the method is suitable for application with slip-ring induction motors since the shape of the T/n curves can be modified, and the braking time reduced, by adding external resistances in the rotor circuit.

6. Discussion and Conclusions

The presented triple-pole braking method for cage induction motors, and the other three methods presently in use have been individually investigated. It remains now to see where the presented method stands in comparison with the others.

1) The most important consideration is probably the energy involved in the rotor and motor circuits during the process of braking. *Table 1* summarizes the previously obtained results.

Obviously, the second and fourth methods are associated with the largest consumption of electrical energy, and the presented triple-pole method is the most economical. With this method, the speed will be brought down to $(n_1/3)$, then the AC supply is switched off, and instantly the mechanical

Table 1.

Braking method	Energy dissipated in rotor circuit	%	Notes
1) Triple-pole	$0.64\ En_1$	100	From n_1 to $\frac{n_1}{3}$
2) Plugging	$3.0\ En_1$	469	From n_1 to $n = 0$
3) DC Dynamic	$1.0\ En_1$	156	From n_1 to $n = 0$
4) Siemens' connection	$3.09\ En_1$	483	From n_1 to $\frac{n_1}{3}$

brake is applied to dissipate the small residual energy ($En_1/9$) in order to stop the motor. Notably, such small energy will not cause any appreciable or quick wear of the mechanical brake, besides there is no danger of reversal. As for cost, the mechanical brake is practically applied with all methods of braking. Furthermore, the triple-pole method is characterized by simplicity since it only requires a switch to change over the connection of the stator phases from normal to triple-pole position.

2) The braking periods, as calculated above, were found as follows for the test motor

Table 2.

Braking method	Time, seconds	Notes
1) Triple-pole	5.0	From n_1 to $\frac{n_1}{3}$
2) Plugging	3.84	From n_1 to $n = 0$
3) DC Dynamic	40.0	From n_1 to $n = 0$
4) Siemens' connection	62.0	From n_1 to $n = 0$

Obviously, the quickest method is plugging, but the time is too short and makes it extremely difficult to apply the mechanical brake at the proper instant by using a "plugging switch", to avoid reversal of rotation. In consequence, in most cases full-voltage plugging is not practicable, and a transformer will then be necessary to apply reduced voltage plugging. But still then top care is required to adjust the plugging switch, besides, the mechanical brake will require the closest maintenance and adjustment, and suffer from rapid wear. It follows that braking by plugging is costly and extravagant.

3) Regarding the method of DC dynamic braking, clearly it removes the danger of reversal of rotation. But the method is unsuitable for cage motors since the braking torque is very low almost in the whole speed range from synchronous speed to standstill. The stopping period is generally too

long, and there may be danger of rebounding with high DC braking currents [7], causing danger to mechanical parts and commodities. The performance with this method may be improved with slip-ring motors by adding appropriate rotor resistances, which, of course, is not possible with cage motors. Furthermore, a special DC source is necessary which is usually obtained by power electronic devices. This adds up to the cost and space requirements, and causes complexity in switching; besides, it brings about harmonics and other problems associated with such devices [3,8].

4) As for Siemens' braking connection, it is noted that the energy dissipated in the rotor circuit from full speed to one-third of this speed, is almost five times the energy necessary with triple-pole braking. Besides, the braking time with this connection is too long to be accepted. In fact, this asymmetrical braking method is suitable only for slip-ring motors for which both the T/n curves and the braking period can be adjusted by rotor resistances added externally.

5) As mentioned in section (2.1), the available test motor happened to be a 2-cage one; the multi-cage design is not a necessity from the viewpoint of triple-pole braking, but obviously it may be utilized to meet special starting regulations or load requirements. Other types of cage motors expectedly yield favourable conclusions which are in essence similar to the above ones. This is confirmed by the triple-pole T/n curve shown in *Fig. 15* for a deep-bar motor of the same ratings as the 2-cage test motor; it is observed that this curve is quite similar to *Fig. 6* of the test motor. It is also recollected here that the comparison of the major point of energy dissipation during braking by the methods considered, *Table 1*, is based on generalized formulae derived in this paper.

All facts pointed out in the above investigation are in favour of the presented triple-pole braking method characterized by security, simplicity, economy, and least consumption of electric energy. Besides, it provides a good and applicable braking method for cage motors, for which other methods like DC dynamic of Siemens' asymmetrical connection are not practicable.

Acknowledgements

The authors acknowledge with thanks of facilities provided by the Electrical Engineering, Power Department of Cairo University.

References

[1] ALGER, P. L.: The Nature of Polyphase Induction Motors, Wiley, 1971, USA.
[2] ABDEL-HAMID, M. N.: Magneto-Motive-Forces of Three-Phase Cage Induction Motors, *Acta Technica Hungarica*, Vol. 58, Hungary.

[3] EMANUEL, A. E.: Survey of Harmonic Voltages and Currents at Customers'Bus, *IEEE Trans. (Power Delivery)*, 1993, USA.
[4] HARRISON, D.: The Dynamic Braking of Induction Motors, *Proc. IEE, (103 A)* London.
[5] HSU, J.: Possible Errors in Measuring of Torques of Induction Motors, *IEEE Trans. (Energy Conversion)*, 1992, USA.
[6] ROGERS, G.: Demystifying Induction Motor Behavior, *IEEE (Computer Appl.)*, 1994, USA.
[7] SHERKAT, V.: The Impact of Dynamic Braking on Shaft Torques, *IEEE Trans(PAS)*, USA, 1980.
[8] YACAMMI, R. – CHANG: Noise and Vibration from Induction Machines Fed from Harmonic Sources, *IEEE Trans (Energy Conversion)*, USA, 1995.
[9] AIEE Committee Report: Stray – Load Loss Measurement in Induction Machines, *AIEE Transactions (Power, Apparatus and Systems)*, April 1959, USA.

Appendix

Test Motor Ratings and Parameters

Ratings

Type	=	3-phase, 2-cage
Kilowatt	=	5 kW
Voltage, star	=	380 Volt
Current	=	12 Ampere
Frequency	=	50 Hz
Number of poles	=	6
Speed	=	965 rpm

Parameters of Equivalent Circuits on Normal and Triple-Pole Operations (per phase, r.t. stator)

	Normal	*Triple-Pole*
Stator resistance, Ohm	$R_1 = 0.8$	$R_1 = 0.8$
Stator leakage reactance	$X_1 = 1.8$	$X_1 = 1.8$
Magnetizing reactance	$X_m = 52$	$X_{m3} = 2.79$
Rotor common reactance	$X_{2c} = 1.8$	$X_{2c3} = 1.2$
Resistance of outer cage	$R_o = 2.49$	$R_{o3} = 1.201$
Resistance of inner cage	$R_i = 0.613$	$R_{i3} = 0.295$
Reactance of inner cage	$X_i = 2.92$	$X_{i3} = 1.409$

INDEX